INSTITUTE OF PHYSICS PUBLISHING NANOTECHNOLOGY
Nanotechnology **17** (2006) 5573–5576 doi:10.1088/0957-4484/17/22/008

Fabrication and field emission property of a Si nanotip array

G S Huang[1,2], X L Wu[1,4], Y C Cheng[1], X F Li[1], S H Luo[2,3], T Feng[3] and Paul K Chu[2]

[1] National Laboratory of Solid State Microstructures and Department of Physics, Nanjing University, Nanjing 210093, People's Republic of China
[2] Department of Physics and Materials Science, City University of Hong Kong, Kowloon, Hong Kong
[3] Shanghai Institute of Microsystem and Information Technology, Chinese Academy of Science, Shanghai 200050, People's Republic of China

E-mail: hkxlwu@nju.edu.cn

Received 16 August 2006, in final form 22 September 2006
Published 25 October 2006
Online at stacks.iop.org/Nano/17/5573

Abstract
Using a Si-based porous anodic alumina membrane as a mask, we demonstrate a way to pattern Si surface. After removing the SiO_2 nanoislands formed during anodization of the Al/Si interface, we obtain a Si nanotip array on the surface of a Si wafer. This array shows an excellent field emission property with a low turn-on field of 8.5 V μm^{-1}. The Fowler–Nordheim plot obtained is linearly dependent, indicating that the emission current arises from the quantum tunnelling effect. The Si nanotip array can be expected to have important applications in nanoelectronic devices.

(Some figures in this article are in colour only in the electronic version)

1. Introduction

Motivated by the fast development of microelectronic miniaturization, semiconductor nanostructures have attracted increasing interest in recent years due to their important applications in electronics, optics, and magnetics [1–3]. Ordinary techniques used in fabricating functional semiconductor nanostructures are nanolithography, including electron lithography, dip-pen lithography, and micro-contact printing [4]. However, these techniques are costly and time consuming with very low output. Recently, more attention has focused on porous anodic alumina membrane (PAAM) because of its favourable applications as a template in fabricating nanostructured materials [5–7]. PAAM formed on Si substrate may be used in integrated-circuit-compatible nanodevices and thus becomes the focus of many investigations [8–10]. In most current studies, Si-based PAAM is only simply used as a host for producing Si-based nanostructured materials and devices [11, 12], whereas transfer of the self-organized nanopore arrangement to the underlying Si substrate to form a nanopatterned Si surface is seldom involved [13–15]. In this paper, we use Si-based PAAM as a mask to pattern Si substrate. By removing the SiO_2 nanoislands formed during anodization of the Al/Si interface, we obtained a Si nanotip array that has excellent field emission characteristics. This type of Si tip array can be expected to have important applications in nanoelectronics.

[4] Author to whom any correspondence should be addressed.

2. Samples and experiments

⟨100⟩-oriented n-type silicon wafer with a resistivity of 5 Ω cm was used as the substrate. Al membrane with a thickness of ∼1000 nm was thermally evaporated onto the Si wafer. Before anodization, the Si-based Al membrane was annealed at 400 °C in N_2 for 30 min to improve the Al–Si bonding at the interface [8]. Anodization was carried out in 0.3 M sulfuric acid under 25 V. The electrolyte was maintained at 5 °C by placing the electrolytic bath in a refrigerator and mechanically stirred. To obtain a Si-based SiO_2 island array, a real-time-controlled anodic method was used with the help of monitoring the anodic current density (J)–time (t) curve (figure 1(a)) [8, 10]. The anodic process lasted a further 300 s after the Al was exhausted (at point X in figure 1(a)). Then the PAAM was removed by putting the sample into a dilute phosphoric acid solution. The morphology and microstructure of the resultant product were characterized

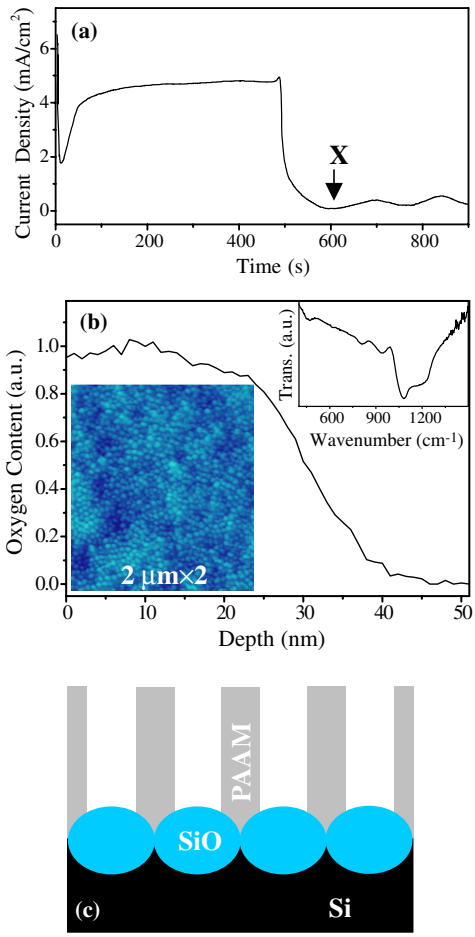

Figure 1. (a) The J–t curve of the anodic process of Si-based PAAM. (b) XPS depth profile of oxygen content in the SiO_2 nanoisland sample. The lower left inset shows an AFM image of the sample. The upper right inset displays the corresponding FTIR spectrum. (c) Structural diagram of Si-based PAAM.

using an atomic force microscope (AFM, Digital Instruments Nanoscope IIIA, working in contact mode using a commercial Si_3N_4 cantilever, with a spring constant of 0.58 N m^{-1} and a tip size of 5–10 nm), x-ray photoelectron spectroscopy (XPS, Physical electronics PHI 5802), and Fourier transfer infrared spectroscopy (FTIR, Nicolet NEXUS870). The field emission characteristics were studied at room temperature in a test chamber with a base vacuum better than 5×10^{-6} Pa. The sample was fixed on a stainless-steel support to serve as a cathode. A parallel phosphor screen located at a distance of 200 μm served as an anode.

3. Results and discussions

An island-like morphology of the sample surface after removing the PAAM can be observed, as shown in the lower left inset of figure 1(b) (AFM image). These nanoislands distribute on the entire substrate surface and have almost an identical diameter of ∼50 nm and an average height of ∼10 nm. The composition of the nanoislands is determined to be SiO_2 in terms of the analysis on the Si 2p XPS spectrum [15, 16]. From our experiments, it can be judged that the SiO_2 nanoislands are formed during Si anodization under an electric field. We know that in the Al anodizing process, oxygen containing ions O^{2-}/OH^- in the electrolyte drift under the high electric field to the alumina/Al interface and then react with Al atoms to form alumina [17]. When the growth front reaches the Al/Si interface, the Al is exhausted (at point X in figure 1(a)). In this case, the electric field building up at the interface region will drive O^{2-}/OH^- across the interface, and therefore, the anodizing process continues through the formation of anodic SiO_2. The SiO_2 cannot be dissolved in sulfuric acid and thus volume expansion takes place with further anodizing. As a result, domed SiO_2 nanoislands appear on the Al/Si interface at the bottom of each nanochannel. A previous investigation showed that the volume expansion resulting from the formation of the SiO_2 nanoislands will cause the alumina barrier layer to break, allowing the electrolyte to penetrate the alumina/SiO_2 interface [10]. This would cause lateral anodization of Si, which leads to the nanoislands having larger diameters. In addition, due to the inhomogeneous distribution of the electric field at the surface, the SiO_2 nanoislands grow with scalloped heads [13]. Such a geometrical model for the formation of the SiO_2 nanoislands is sketched in figure 1(c). To determine the penetration depth of the oxygen ions on the Si surface under electric field, we carried out an XPS elemental depth profile measurement. Figure 1(b) displays the oxygen content as a function of the depth. One can see that the oxygen content keeps almost unchanged in the initial 20 nm depth, indicating that the height of the SiO_2 nanoislands is about 20 nm. This value is larger than that obtained from the AFM measurements. The difference is considered to be due to the influence of the AFM tip, because relatively large AFM tips can hardly penetrate into the narrow spaces between SiO_2 nanoislands (see figure 1(c)), which leads to a smaller measured height. In the XPS depth profile demonstrated in figure 1(b), an obvious decrease occurs after 25 nm depth and expands to ∼40 nm. This decrease provides good support to our structural model of the SiO_2 nanoislands because the scalloped Si/SiO_2 interface should have a gradual decrease of SiO_2 content with increasing depth (see figure 1(c)). On the basis of the elemental depth profile and our structural model, we may infer that the depth of the SiO_2 nanoislands is ∼40 nm. To go deeper into the bonding structure of the nanoislands, the FTIR spectrum was recorded and is displayed in the upper right inset of figure 1(b), which shows characteristic Si–O asymmetric stretching (1080 cm^{-1}), O–Si–O bending (809 cm^{-1}), and Si–O–Si rocking vibration modes (456 cm^{-1}) [18, 19]. Besides, a broad absorption peak centred at ∼1180 cm^{-1} is noticeable. The origin of this absorption band is still the subject of controversy [20]. In our present case, according to the aforementioned growth process of the SiO_2 nanoislands, it is reasonable to infer that under the electric field, O^{2-} drifts into Si lattices to form interstitials O ions, which produces the 1180 cm^{-1} absorption band [19]. Since this band is rather broad, we can further infer that these interfacial O atoms are at different local structures. This is also consistent with formation mechanism of the SiO_2 nanoislands.

In order to completely remove the SiO_2 nanoislands with a 40 nm depth, we tested the HF concentration and immersing time, and found that this could be achieved by immersing the sample in 1 wt% HF at 20 °C for 15 min. Removal of

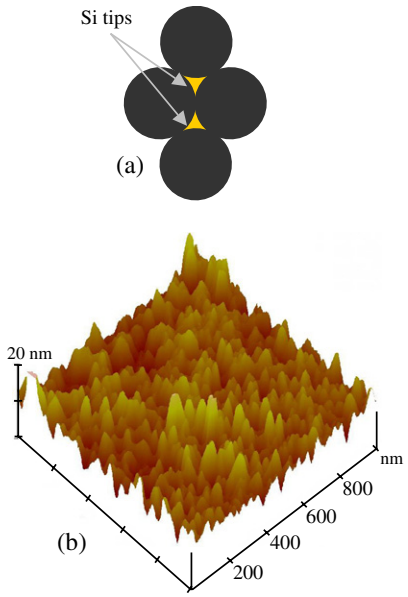

Figure 2. (a) Schematic diagram for the formation of the Si nanotips. The dark circles represent the convexes, which will be left after removing the SiO_2 nanoislands. (b) 3D AFM image of the Si nanotip array.

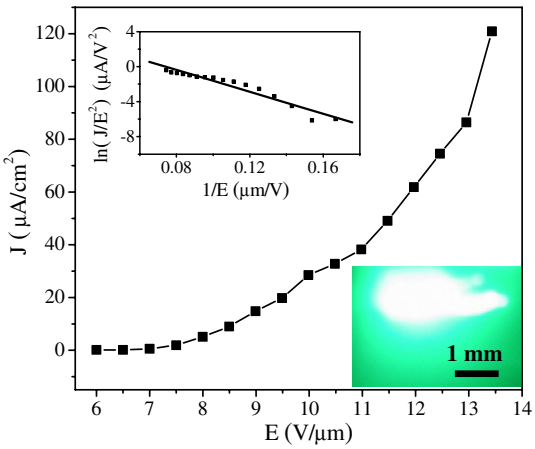

Figure 3. J–E curve of the field emission property of the Si nanotip array. The upper left inset displays the FN plot. The dark squares are the experimental data and the solid line is a result of linearly fitting the experiment data. The lower right inset shows a luminescent spot on the anode at an emission field of 9.5 V μm^{-1}.

the SiO_2 nanoislands will leave Si tips at the triple points of the SiO_2 nanoislands, as shown in figure 2(a). As a result, a Si nanotip array is formed on the Si surface. The density of the SiO_2 nanoislands determines that of the Si nanotips. Figure 2(b) shows an AFM image of the tip array. The tips have bottom diameters of 20–30 nm and heights of ∼20 nm. The sharpness of the Si nanotips obviously suggests potential application of the nanotips as electron emitters. To prove this assumption, the field emission characteristics of the nanotip array were measured and the exponential dependence of the emission current density (J) on the applied electric field (E) is displayed in figure 3. The turn-on field is determined to be as low as 8.5 V μm^{-1} (defined as the electric field to extract a current density of 10 $\mu A\ cm^{-2}$). The lower right inset of figure 3 demonstrates the distribution of a luminescent spot on the anode at an electric field of 9.5 V μm^{-1}. The brightly and evenly luminescent spot indicates an excellent field emission property of the sample with homogeneous Si nanotips. Here, the field emission property is further evaluated by the Fowler–Nordheim (FN) equation [21–23],

$$J = (A\beta^2 E^2/\phi)\exp(-B\phi^{3/2}/\beta E), \qquad (1)$$

where β is the field enhancement factor, ϕ is the work function of the electron emitter, and A and B are constants with the values of 1.56×10^{-10} A V^{-2} eV and 6.83×10^3 V $eV^{-3/2}$ μm^{-1}, respectively. The corresponding FN plot $[\ln(J/E^2) - 1/E]$ is demonstrated in the upper left inset of figure 3. Good consistency between the experimental data (dark square) and linear fitting (solid line) shows that the emission current originates from the quantum tunnelling effect (FN tunnelling) [22, 23]. From equation (1), the electron emission current is determined by two parameters: ϕ and β. Generally, bulk crystal Si with a relatively large work function ϕ is not a good electron emission material. Therefore, the present field emission property should be ascribed to the influence of β, which is an important parameter reflecting the true value of the electric field at the Si nanotips [21]. The value of β can be calculated from the slope of the FN plot. It can be derived from equation (1) to be $-B\phi^{3/2}/\beta$. Using the pure Si work function of 4.7 eV, we can roughly estimate β to be as large as 1100 for our current nanotip array. Since β depends upon $1/r$ (r is the curvature radius of the tip end) [24], the large field enhancement factor is intimately connected with the unique structure of the Si nanotips. Although an exact size of the tip end cannot be reflected in our AFM observations, the Si tips located at the triple points can still be observed to be very sharp (figure 1(c)), which is responsible for the remarkable increase of β. Furthermore, it is known that the surface bonding structure of a nanotip has a large influence on the field emission property [22, 24]. The present Si nanotips are fabricated by chemical etching in a dilute HF solution. This removes the insulating oxide surface which can cause electron accumulation and thus leads to enhancement of the field emission current. In addition, the single crystal nature of the Si nanotips and their good contact with the underlying Si substrate can also effectively reduce the impedance produced by electron scattering at the tip boundary. As a result, the field emission current can be further promoted.

4. Conclusions

We have fabricated a Si nanotip array by using Si-based PAAM as a mask. This array is obtained by removing the SiO_2 nanoislands formed during anodization of the Al/Si interface. Due to the unique surface structure and morphology, the Si nanotip array exhibits excellent field emission characteristics with a low turn-on field of 8.5 V μm^{-1} and a large field enhancement factor of ∼1100. Linear dependence of the FN plot reveals the quantum tunnelling mechanism of the emission current. This type of Si nanotip array can be expected to have important applications in nanoelectronic devices.

Acknowledgments

This work was supported by grants (Nos 10225416, 60476038, and BK2006715) from the National and Jiangsu Natural Science Foundations and the LAPEM. Partial support was also received from the Major State Basic Research Project No. G001CB3095 of China and the City University of Hong Kong Direct Allocation Grant No. 9360110.

References

[1] Cho K H, Choi B H, Son S H, Hwang S W, Ahn D, Park B G, Naser B, Lin J F and Bird J P 2005 *Appl. Phys. Lett.* **86** 043101
[2] Tewary A, Kekatpure R D and Brongersma M L 2006 *Appl. Phys. Lett.* **88** 093114
[3] Yang L W, Wu X L, Qiu T, Siu G G and Chu P K 2006 *J. Appl. Phys.* **99** 074303
[4] Yun Y J, Park G, Ah C S, Park H J, Yun W S and Ha D H 2005 *Appl. Phys. Lett.* **87** 233110
[5] Masuda H and Fukuda K 1995 *Science* **268** 1466
[6] Li J, Papadopoulos C and Xu J 1999 *Nature* **402** 253
[7] Kouklin N, Menon L, Wong A Z, Thompson D W, Woollam J A, Williams P F and Bandyopadhyay S 2001 *Appl. Phys. Lett.* **79** 4423
[8] Huang G S, Wu X L, Xie Y, Shao X F and Wang S H 2003 *J. Appl. Phys.* **94** 2407
[9] Krishnan R, Nguyen H Q, Thompson C V, Choi W K and Foo Y L 2005 *Nanotechnology* **16** 841
[10] Kimura Y, Shiraki H, Ishibashi K, Ishii H, Itaya K and Niwano M 2006 *J. Electrochem. Soc.* **153** C296
[11] Mei Y F, Siu G G, Yang Y, Fu R K Y, Hung T F, Chu P K and Wu X L 2004 *Acta Mater.* **52** 5051
[12] Sander M S and Tan L S 2003 *Adv. Funct. Mater.* **13** 393
[13] Pu L, Shi Y, Zhu J M, Bao X M, Zhang R and Zheng Y D 2004 *Chem. Commun.* **8** 942
[14] Asoh H, Matsuo M, Yoshihama M and Ono S 2003 *Appl. Phys. Lett.* **83** 4408
[15] Kokonou M, Nassiopoulou A G, Giannakopoulos K P, Travlos A, Stoica T and Kennou S 2006 *Nanotechnology* **17** 2146
[16] Huang G S, Wu X L, Mei Y F, Chen P and Chu P K 2004 *J. Appl. Phys.* **96** 1443
[17] Huang G S, Wu X L, Mei Y F, Shao X F and Siu G G 2003 *J. Appl. Phys.* **93** 582
[18] Andrés E S, del Prado A, Martínez F L, Mártil I, Bravo D and López F J 2000 *J. Appl. Phys.* **87** 1187
[19] Hu Q, Suzuki H, Gao H, Araki H, Yang W and Noda T 2003 *Chem. Phys. Lett.* **378** 299
[20] Arnoldbik W M, Tomozeiu N, van Hattum E D, Lof R W, Vredenberg A M and Habraken F H P M 2005 *Phys. Rev.* B **71** 125329
[21] Xu C X, Sun X W, Fang S N, Yang X H, Yu M B, Zhu G P and Cui Y P 2006 *Appl. Phys. Lett.* **88** 161921
[22] Luo S H, Chu P K, Di Z F, Zhang M, Liu W L, Lin C L, Fan J Y and Wu X L 2006 *Appl. Phys. Lett.* **88** 013109
[23] Huang A P, Chu P K and Wu X L 2006 *Appl. Phys. Lett.* **88** 251103
[24] Lebedev V, Morales F M, Fischer M, Himmerlich M, Krischok S, Schäfer J A and Ambacher O 2006 *Phys. Status Solidi* a **203** 1839